EFFECT OF IRON DOPING ON STRUCTURAL AND OPTICAL PROPERTIES OF TIO_2 THIN FILM BY SOL-GEL SPIN COATING TECHNIQUE

Lourduraj S [1], Victor Williams R*
PG and Research Department of Physics,
St. Joseph's College (Autonomous),
Tiruchirappalli.

Abstract

Thin films of iron (Fe) doped titanium dioxide (Fe:TiO_2) were prepared on a glass substrate by sol–gel spin coating technique and further calcined at 450°C. The Structural and optical properties of Fe doped TiO_2 thin films were investigated by X-ray diffraction (XRD), scanning electron microscopy (SEM), ultraviolet–visible spectroscopy (UV–vis) and Atomic force microscopic (AFM) techniques. The XRD results confirm the nanostructured TiO_2 thin films having crystalline nature with anatase phase. The characterization results shows that the calcined thin films having high crystallinity and the effect of iron substitution leads to decreased crystallinity. The SEM investigations of Fe doped TiO_2 films also gave evidence that the films were continuous spherical shaped particles with a nanometric range of grain size and film was porous in nature. AFM analysis establishes that the uniformity of the TiO_2 thin film with average roughness values. The optical measurements show that the films having high transparency in visible region and the optical band gap energy of TiO_2 with ion (Fe^{3+}) doping decreases with increase in iron content. These important requirement for the Fe:TiO_2 films to be used as window layer in solar cells.

Keywords: TiO_2 thin film, Fe doped TiO_2 thin film, sol-gel method, spin coating, calcination.

Introduction

In research and development, the TiO_2 will become an important wide band gap semiconductor and photoelectric conversion material. TiO_2 coating has been investigated by many researchers because TiO_2 is stable, nontoxic with band gap of 3.21 eV making it possible for photovoltaic[1] and photo catalytic[2] application. It is well known TiO2 nanoparticles with good physico-chemical properties are mainly dominated by three phases namely anatase, rutile and brookite. On a nanometer scale or in a thin layer form, TiO_2 nanoparticles are transparent and have a wide surface area[3]. To improve the performance of TiO_2 thin film for photovoltaic application such as dye sensitized solar cell, TiO_2 layer has been modified by the adding metal ions dopant such as Fe [4] and Zn [5]. It is also reported that to improve the crystal size of TiO_2, treatment such as by optimizing dopant concentration of the precursor can be performed [6].

Many applications of TiO_2 thin film is at the basis of fundamental properties that relate to surface and interface features of the film. A wide range of metal ions, in particular transition metal ions such as iron [7], chromium [8] and cobalt [9], have been used as dopants for TiO_2 with the intention of improving photovoltaic and extending absorption into the visible light range. Iron (Fe) has been the most widely examined among these elements.

Fe-doped TiO_2 thin films can be prepared by several techniques, including sol–gel [10], reactive sputtering [11], pulsed laser deposition [12], evaporation [13], chemical vapor deposition [14], and spray

pyrolysis [15] etc... The sol-gel technique has emerged as one of the most promising method as it produces samples by simple synthetic route with good homogeneity, low cost, excellent compositional control and feasibility of producing thin films on large complex shapes with low crystallization temperature.

In the present work, Fe-doped TiO_2 films were deposited on glass using sol-gel spin coating technique. The effect of the Fe dopant on the structural, morphological and optical properties of the resultant TiO_2 thin films useful to photovoltaic applications in solar cells.

2. Experiment

2.1. Materials

The precursors used in the preparation of Fe doped TiO_2 film by sol-gel spin coating technique were Titanium tetra isopropoxide (TTIP, 98%), isopropanol (98%) for dopant Ferric oxide (98%), methanol (97%), and hydrochloric acid (97%) from Sigma Aldrich Co. Ltd. The glass plate is used as a substrate.

2.2. TiO_2 film preparation

Nano crystalline un-doped TiO_2 and Fe doped TiO_2 thin films were deposited on glass substrates using sol-gel spin coating method. The sol is based on the hydrolysis of alkoxide in alcoholic solution in the presence of an acid catalyst. Titanium isopropoxide (TTIP) ($Ti(OCH(CH_3)_2)_4$ is used as the TiO_2 precursor while isopropanol ($CH_3CH(OH)–CH_3$), ethanol (CH_3OH) and hydrochloric acid (HCl) is used as solvent and catalyst respectively. The procedure of preparation includes the dissolution of methanol, isopropanol as solvent and hydrochloric acid, titanium isopropoxide is also added as precursor after mixing for 24 h the adequate proportions. A schematic flow chart of the Fe - doped TiO_2 thin films prepared by a sol–gel spin coating process is shown in Fig. 1. We obtain at the final a transparent solution of yellowish color and ready for the deposit. The dopant solution for Fe doped TiO_2 thin film were prepared with different atomic weight percentage of Fe concentration and is defined as $x= [Fe/(Ti+Fe)]\times100$. After stirring at room temperature for 24 h, the Fe doped TiO_2 sols were Spin-coated on glass substrate. Spin coating process was done by dropping ~ 0.2 mL of solution onto glass substrates spun in air for 60 s at 4500 rpm. Instantaneous heating at 100^oC for 30 min was following this spin coating process. Subsequently calcination was carried out using a furnace at 450^oC for an hour.

2.3. Characterization of TiO_2 film

The X-ray diffraction (XRD) analysis was carried out for identifying the crystal phase with a XPERT-PRO X-ray diffractometer with Cu K_α radiation in the range of 2 theta values from 20° to 80° (λ = 0.1540nm). The structural characteristics of TiO_2 films were analyzed by VEGA3 TESCAN scanning electron microscope and Atomic force microscope (AFM XE-100). The properties of the films deposited on glass substrates were examined with the normal incident transmittance measured by a UV–VIS spectrophotometer (Lambda 35 UV/Vis (Perkin Elmer)).

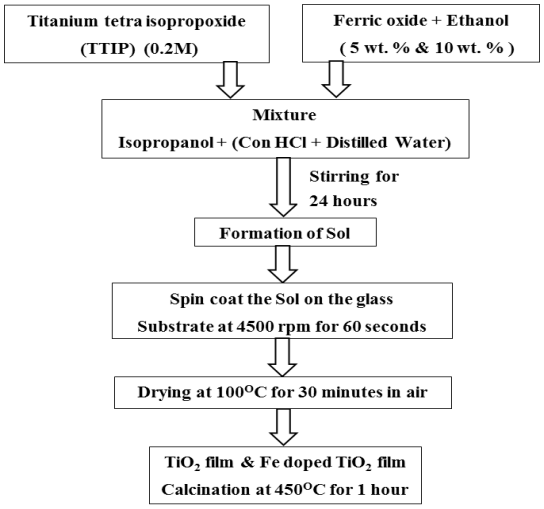

Fig. 1: Flow chart of the TiO_2 and Fe-doped TiO_2 thin films prepared by a sol–gel spin coating process.

3. Result and discussion

3.1. X-ray diffraction analysis

X-ray diffraction patterns of Fe^{3+} doped TiO_2 thin films calcined at 450°C for 1 h are shown in Fig. 2. The diffraction pattern exhibits characteristic peaks (anatase) corresponding to 2 theta values 25, 37, 48, 53, and 62 as (110), (004), (211), (200), and (204) respectively. The crystalline nature (tetragonal) and purity of the sample are confirmed by comparing the data with JCPDS (card No: 04-0477) data. The width of peak of anatase to became narrower. This was due to the enhancement of crystallization and the growth of crystallites. The result reveals that the intensity of diffraction peak decreases with an increasing Fe^{3+}-dopant concentration. This phenomenon caused by the Fe^{3+}-doped TiO_2 film can exhibit the crystallization of anatase TiO_2. The average crystallite size of the TiO_2 thin films with Fe^{3+}-doped concentrations (5 wt. % and 10 wt. %) calcined at 450°C determined, by the Scherrer's equation [16]. The size of TiO_2 thin films decreases from 24.1 to 7.8 nm when the Fe^{3+} doped concentration increases from 5 wt.% to 10 wt.% [17].

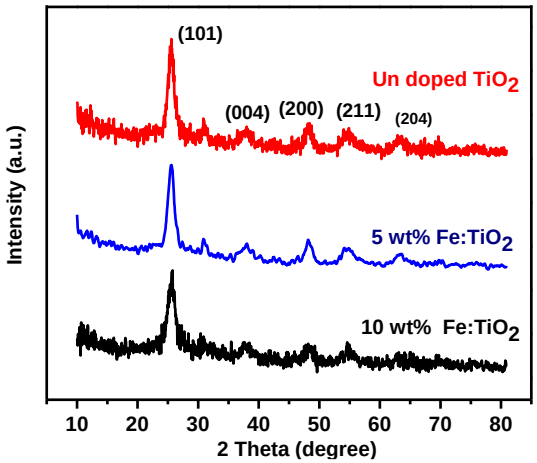

Fig.2. X-ray diffraction pattern of Fe doped TiO_2 thin film calcined at 450°C

3.2. Surface morphological analysis

3.2.1. Scanning Electron Microscopy Analysis

The SEM micrographs (Figure 3) of TiO_2 and 5 wt.% and 10 wt.% of Fe doped TiO_2 films were prepared and calcined at 450°C exhibit that the particles are spherical in shape and are nanostructured. The TiO_2 films having smooth in surface and porous in nature [18].

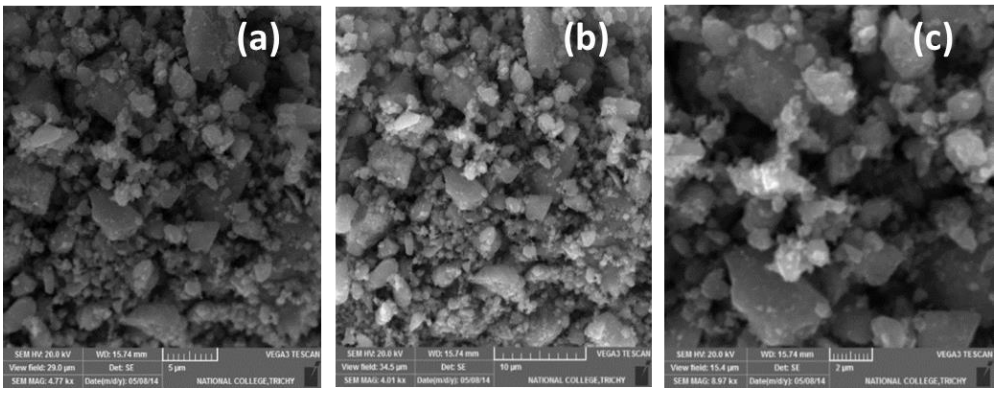

Fig.3. SEM images of (a) un-doped and (b) Fe 5 wt.% and (c) Fe 10 wt.% doped TiO_2 thin films calcined at 450°C.

3.2.2. Atomic force Microscopy analysis

The topography images of un-doped and Fe doped TiO_2 films (Figures 4. a, b and c) in tapping mode confirms the uniform distribution of smooth and spherical-shaped particles [19]. The average roughness values of the all TiO_2 films were found to be 15.4nm.

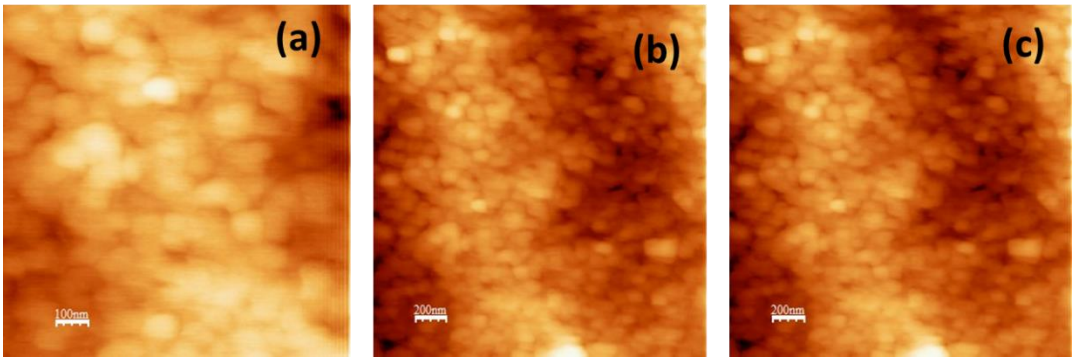

Fig.4. AFM images of (a) Un doped and (b) Fe 5 wt. % and (c) Fe 10 wt. % doped TiO_2 thin films calcined at 450°C.

4. Optical analysis

The UV–Vis transmittance and absorbance spectra of un-doped and Fe doped TiO_2 thin films are shown in Fig. 5 (a & b). The transmittance spectrum of the prepared TiO_2 films shows that, in both the UV (400 nm) and visible (400– 800 nm) regions film having high transparency and it decreased with increasing Fe dopant concentrations [20]. The absorbance spectrum of the prepared TiO_2 films

shows that the absorption edge shifted towards longer wavelengths (red shifted) from 345 to 380 nm with the Fe -doped concentration increasing from 5 to 10 wt. %. Red shift associated with the presence of dopants can be attributed to a charge transfer transition between the iron d-electrons and the TiO_2 conduction or valence band. The porosity values of TiO_2 thin films increases with increasing the concentration of iron doping [21].

Fig.6 illustrates the plot of (hν) vs. $(\alpha h\nu)^{1/2}$ thin films with various Fe^{3+} for the TiO_2 contents. From the intersection of the extrapolation of each curve in Fig.6 and hν axis gives the band-gap energy of TiO_2 thin films with different Fe^{3+} doping concentrations. It reveals that the band-gap energy decreases when the Fe content increases [22, 23].

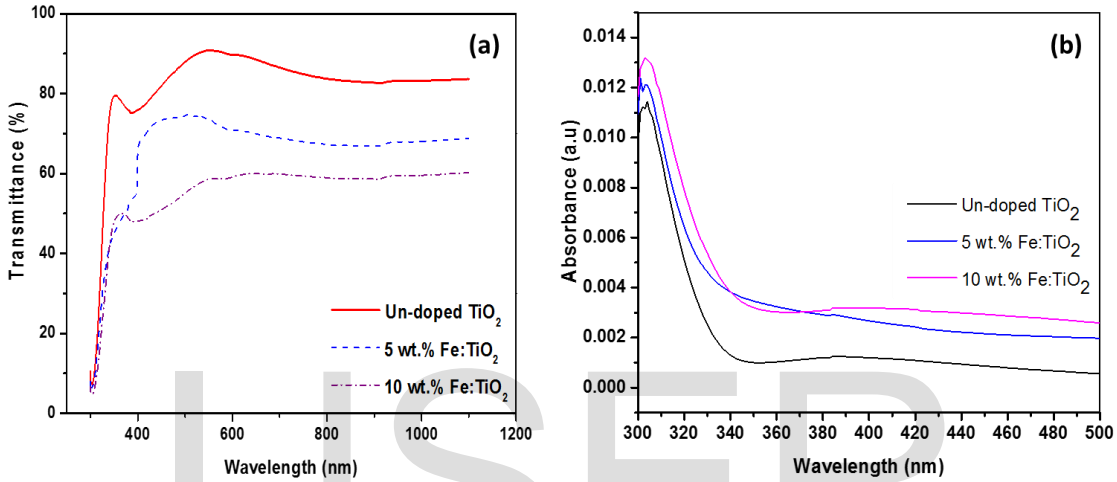

Fig.5. UV-vis (a) Transmittance and (b) Absorbance spectra of un-doped, Fe 5 wt. % and Fe 10 wt. % doped TiO_2 thin films calcined at 450°C.

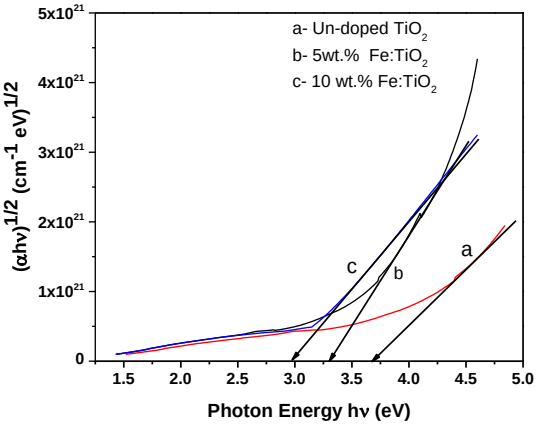

Fig.6. Optical band gap energy of un-doped, 5 wt. % Fe:TiO_2 and 10 wt. % Fe:TiO_2 thin films calcined at 450°C.

Conclusion

The nanostructured titanium dioxide (TiO_2) and Fe doped TiO_2 thin films were prepared using the sol-gel routed spin coating technique. TiO_2 thin films are crystallized as anatase phase and are nanostructured with tetragonal system. The grain size of TiO_2 thin films decreases from 24.1 to 7.8 nm when the Fe^{3+} doped concentration increases from 5 wt.% to 10 wt.%. The SEM images exhibit that the particles are spherical in shape. TiO_2 and Fe:TiO_2 thin films having smooth in surface and porous in nature. The porosity values of TiO_2 thin films increases with increasing the concentration of iron doping. The average roughness values of the TiO_2 films were found to be 15.4nm. The optical transmittance is found to be the film having high transparency and it was decreased with increasing Fe dopant concentrations. The absorbance spectrum of the prepared TiO_2 films shows that the absorption edge shifted towards longer wavelengths (red shifted) from 345 to 380 nm with the Fe -doped concentration. The band-gap energy decreases with increase in Fe content will be useful to photovoltaic application due to its structural and optical behavior.

References

1. G. Liu, J. C. Yu, G. Q. M. Lu, and H.-M. Cheng, Crystal facet engineering of semiconductor photocatalysts: motivations, advances and unique properties, *Chem. Commun, (Camb)*, 47, 6763–6783, (2011).
2. A. A. Umar, M. YA. Rahman, S. K. M. Saad, and M. M. Salleh, Effect of NH3 Concentration on the Performance of Nitrogen doped TiO2 Photoelectrochemical Cell, *Int J Electrochem Sci*, 7, 7855–7865, (2012).
3. M. Ouzzine, J. A. Macia-Agullo, M. A. Lillo-Rodenas, C. Quijada, and A. Linares-Solano, Synthesis of high surface area TiO2 nanoparticles by mild acid treatment with HCl or HI for photocataytic propene oxidation, *Applied Catalysis B Environmental*, (2014).
4. B. Kilic, N. Gedic, S. P. Mucur, and A. S. Hergul, Band gap engineering and modifying surface of TiO2 nanostructures by Fe2O3 for enhanced-performance of dye sensitized solar cell, *J. Mater Sci. Smiconductor Process*, 31, 363–371, (2015).
5. S. K. M. Saad, A. A. Umar, M. Y. A. Rahman, and M. M. Salleh, Porous Zn-doped TiO2 nanowall photoanode: effect of Zn2 concentration on the dye-sensitized solar cell performance, *Appl Surf Sci*, 353, 835–842, (2015).
6. H. I. Hsiang and S. C. Lin, Effect of aging on nanocrystalline anatase-to-rutile phase transformation kinetics, *Ceram Int*, 34, 557–561, (2008).
7. K.T. Ranjit, B. Viswanathan, J. Photochem. Photobiol. A: Chem. 108 (1997)79.
8. J.A. Navio, G. Colon, M. Macias, C. Real, M.I. Litter, Appl. Catal. A: General 177 (1999) 111.
9. M.I. Litter, J.A. Navio, J. Photochem. Photobiol. A: Chem. 98 (1996) 171.
10. C.J. Brinker, M.S. Harrington, Sol–gel derived antireflective coatings for silicon, Solar Energy Mater, 5 (1981) 159–172.
11. T.M.R. Viseu, M.I.C. Ferreira, Vacuum 52 (1999) 115.
12. Y. Suda, H. Kawasaki, T. Ueda, T. Ohshima, Thin Solid Films 475 (2005) 337.

13. M. Lottiaux, C. Boulesteix, G. Nihoul, Thin Solid Films 170 (1989) 107.
14. K.S. Yeung, Y.W. Lam, Thin Solid Films 109 (1983) 169.
15. I. Oja, A. Mere, M. Krunks, R. Nisumaa, C.H. Solterbeck, M. Es-Souni, Solid Films 515 (2006) 674.
16. E. Borgarello, J. Kiwi, E. Pelizzetti, M. Visca, M. Graetzel, J. Am. Chem. Soc. 103 (1981) 6324.
17. M. Zhou, J. Yu, B. Cheng, H. Yu, Mater. Chem. Phys. 93 (2005) 159.
18. M.C. Wang et al. Journal of Alloys and Compounds 473 (2009) 394–400.
19. D.A.H. Hanaor, C.C. Sorrell, Review of the anatase to rutile phase transformation, J. Mater. Sci. 46 (2011) 855–874.
20. D.H. Kim, H.S. Homg, S.J. Kim, J.S. Song, K.S. Lee, J. Alloys Compounds 375 (2004) 259.
21. M. Rosi, F. D. Eljabbar, U. Fauzi, M. Abdullah dan Khairurrijal, "Pengolahan Citra SEM dengan Matlab untuk Analisis Pori pada Material Nanopori", Journal Nanosciene and Nanotechnology, Vol. Edition, Khusus (Aguest), 2009, 29.
22. H.P. Maruska, A.K. Ghosh, Sol. Energy 20 (1978) 443.
23. C. Jia, E. Xie, A. Peng, R. Jiang, F. Ye, H. Lin, T. Xu, Thin Solid Films 496 (2006) 555.